

## VARIABILITY OF PLANETARY MASS COMPANION 2M1207 B

YIFAN ZHOU, DANIEL APAI, ...  
 University of Arizona  
*Draft version August 4, 2015*

### ABSTRACT

...  
*Subject headings:* kw1, kw2, ...

#### 1. INTRODUCTION 2. OBSERVATION

We carried out high contrast direct imaging observation of 2M1207 system on UT 2014 April 11 using HST. (*HST* Proposal GO-13418, PI: D. Apai). The data were acquired with the Wide Field Camera 3 (WFC3, citation needed) in filter F125W and F160W using the  $256 \times 256$  sub-array mode. We observed 2M1207 system in continuous 6 HST orbits and obtained a data-set that have a temporal resolution of  $\sim 1.5$  minutes and baseline of  $\sim 8$  hours.

The observation was initially designed to apply standard roll subtraction to remove the primary star. The telescope roll angles for data taken in orbit 1, 3, 5 and those taken in orbit 2, 4, 6 have a difference of  $25^\circ$ , thus the companion would appear at different position relative to the primary with different roll angle and the primary in the two data set can be subtracted from each other. In each orbit we will take a sequence of 13 SPARS25 exposures with NSAMP=10, alternating between F160W and F125W filters. To improve PSF sampling and reduce the influence of bad pixels, we applied standard 4 point dithering. In each orbit, exposures were taken with dithering position 1 – 4 sequently. To sum, we obtained 70 multi-acuum images for filter F125W and 64 images for filter F160W with exposure time of 88.4 seconds for both two filters.

#### 3. DATA REDUCTION

Through the whole analysis, we used the `flt` files that were produced by WFC3's `calwfc3` pipeline. The `flt` files were reduced with calibrations including dark current correction, non-linearity correction, and flat field correction. A further step of up-the-ramp fit was applied to combine all non-destructive read and remove cosmic rays. Although Mandell et al. stated that WFC3 IR time series extract from `flt` files have a rms 1.3 times larger than that obtained from `ima` files, `flt` files keeps all pixels of the image of 2M1207 A unsaturated while in most of non-destructive reads the cores of 2M1207 A are saturated, so that with `flt` files the flux of 2M1207 B can be more precisely separated from that of 2M1207A.

The small angular separation of 2M1207 A and B (as shown in Figure 1) makes precise primary star subtraction and photometry very difficult. On the under-sampled WFC3 IR detector (plate scale  $\sim 0.13$  arcsec per pixel), the primary and the secondary only separate by  $\sim 6$  pixels, which is about 5 times of the FWHM of the PSF. In addition, under-sampling of the PSF causes

significant artifacts when shifting the PSF to register images no matter what interpolation method is used.

#### 3.1. Tiny Tim PSF Photometry

To over come the difficulty, we make use of the Tiny Tim PSF simulator to pursue high precision photometry under this extreme circumstance. Tiny Tim can produce model PSF based on the filter, spectrum of target, focus status, and the telescope jitter. One significant advantage of Tiny Tim PSF over empirical PSF is that Tiny Tim can produce over-sampled PSF, which makes the shifting and interpolation rather straight forward. However, Tiny Tim model PSFs have systematic errors. Biretta demonstrated that the diffraction spikes and coma are not well simulated with Tiny Tim for WFC3 IR images.

We start the reduction by making bad pixel masks for every images. Pixels with data quality flags 'bad detector pixels' (DQ = 4), 'unstable response' (DQ = 32), and 'bad or uncertain flat value' (DQ = 512) were masked out and excluded from further analysis as suggested by previous transit exoplanet spectroscopic observations (e.g. Berta et al. 2012; Kreidberg et al. 2014).

We then produced a list of 10x over-sampled PSFs based on the positions and spectrum (Bonnefoy et al. 2014) of 2M1207A with different telescope jitter ranging from 0 to 50 mini-arcsec per second in both  $x$  and  $y$  direction. The focus parameter was calculated using the model listed on the STScI website<sup>1</sup>. The PSFs were registered with the original image by searching on a dynamic grid and minimizing the residual of a region centered on 2M1207 A with the image of 2M1207 B mostly excluded. The best fitted primary star position and telescope jitter were obtained in this step. Then, we generated the PSF for 2M1207 B based on its position on detector, spectrum (Patience et al. 2010), and the telescope jitter that had been obtained above. In the final step, we combined the two PSFs together. We fixed the position of the primary as it had been fitted in the first step and fitted for the amplitude of the two PSFs and the precise position of the secondary. Since the total fluxes of the model PSFs are normalized to unity as default, the fluxes of 2M1207 A and B are solely represented by the amplitude of the two PSFs coordinately.

Because of the systematic errors of the Tiny Tim PSF, the quality of the fitting is not optimistic. The reduced  $\chi^2$  values are around  $\sim 10$ . However, we found that the residual patterns were very stable among the im-

<sup>1</sup> <http://www.stsci.edu/hst/observatory/focus/FocusModel>

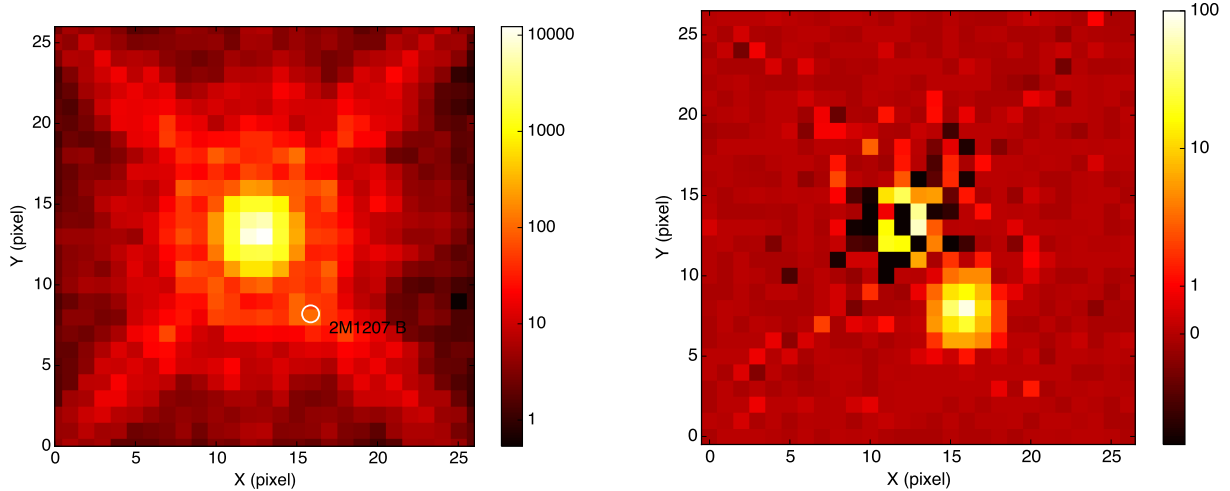


FIG. 1.— WFC3 F160W images of 2M1207A system. Upper: original image, lower: residual model and primary PSF subtracted. The image of 2M1207 B is overshadowed by the halo of the image of 2M1207A and can be hardly seen from the original image. With a hybrid PSF (residual + Tiny Tim PSF) subtraction, the image of 2M1207 B is clearly presented.

age that have the same dithering position and telescope rolling. Therefore, we median combined the residual images that have the same dithering position and telescope rolling angle to construct 8 residual models (4 dithering position  $\times$  2 telescope rolling angle) for each filter. We pre-subtract the corresponding residual from the original image and repeated the procedure that listed above. Using this extra-step, the systematic error of Tiny Tim greatly decreased to around unity.

The fluxes for both 2M1207 A and B are clearly correlated with the dithering position, which is primarily due to imperfection of the flat field. To reduce the correlation, we normalize each group of exposures that have the same dithering position and roll angle individually – we took the median of the fluxes that were measured from these exposures as normalization factors and divided them from every flux measurement.

#### 4. RESULT

We obtained high signal to noise photometry series for both 2M1207 A and B. On average, the photometric contrast is  $6.52 \pm 0.03$  for F125W and  $5.77 \pm 0.02$  for F160W. The difference of F125W contrast from 7.0 magnitude of J-band contrast (Mohanty et al. 2007) and that of F160W contrast from 5.60 magnitude of NICMOS F160W contrast (Song et al. 2006) are due to the different throughput profiles of the filters.

Normalized light curves for both filters are presented in Figure 2. Although the light curves are relative noisy and have a scattering of  $\sim 3\%$ , both F125W and F160W light curves for 2M1207 B demonstrated a significant

time variability.

##### 4.1. Uncertainty analysis

- the source of the scattering –
- flat field uncertainty – adding artificial flat field error mask
- validity of the variability
  - both filter demonstrate similar period of variability
  - split the data into two half, the trend in two halves of data looks similar.
  - fix the position does not change the light curve
- uncertainty of sinusoidal curve fit – carry out a mcmc fit? is it worth doing this.

#### 5. DISCUSSION

- a data-reduction pipeline is developed to obtain high precision photometry measurement from high contrast WFC3 IR data. For a contrast of  $\sim 7$  magnitudes at an angular separation of  $\sim 0.7''$ , we obtained photometry measurement for 2M1207 B at precision of about 2-3%.
- time variability for 2M1207 B was discovered, the light curve of 2M1207 B for both two colors can be fitted with a  $T=10.7$  hr sinusoidal curve.
- the atmosphere and cloud structure of 2M1207 B. How does it compare to the brown dwarf.

#### REFERENCES

- Berta, Z. K., Charbonneau, D., Désert, J.-M., et al. 2012, *ApJ*, 747, 35
- Biretta, J. 2014, *Space Telescope WFC Instrument Science Report*, 1, 10
- Bonnefoy, M., Chauvin, G., Lagrange, A.-M., Rojo, P., Allard, F., Pinte, C., Dumas, C., & Homeier, D. 2014, *A&A*, 562, A127
- Kreidberg, L., Bean, J. L., Désert, J.-M., et al. 2014, *Nature*, 505, 69
- Mandell, A. M., Haynes, K., Sinukoff, E., et al. 2013, *ApJ*, 779, 128
- Mohanty, S., Jayawardhana, R., Huelamo, N., & Mamajek, E. 2007, *ApJ*, 657, 1064
- Patience, J., King, R. R., De Rosa, R. J., & Marois, C. 2010, *A&A*, 517, A76

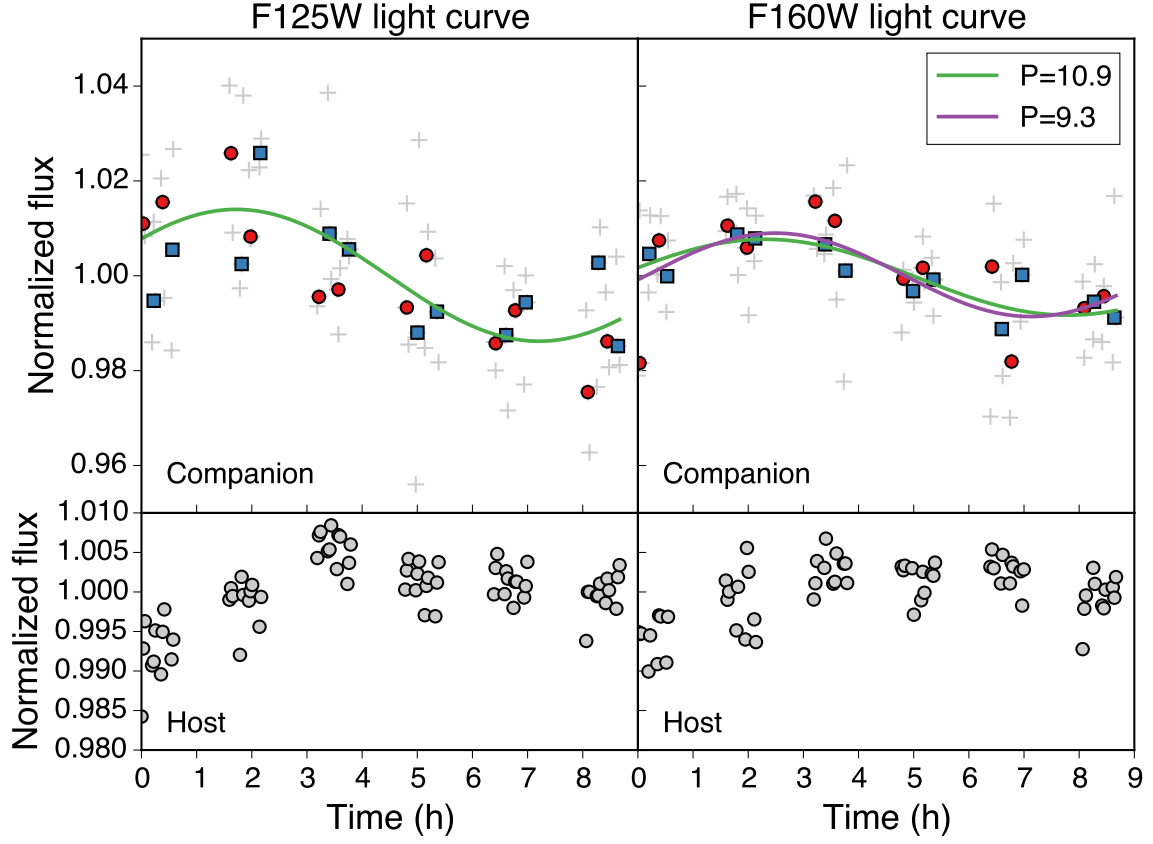


FIG. 2.— Normalized F125W and F160W light curves for 2M1207 B and A. For companion's light curves, gray crosses are unbinned photometric measurements while red circles and blue squares are exposure-set-based binned data representing two halves of the data set. For F160W, green curve is least square fitted sinusoidal wave with period fixed to be same as the fitting result for F125W, and purple curve is the one with no parameter fixed in the fitting routine.

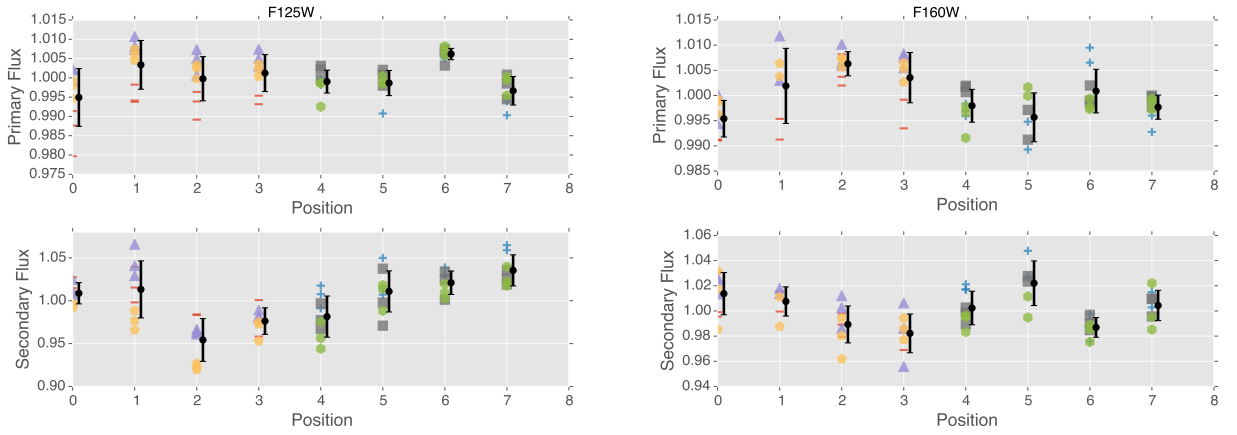


FIG. 3.— Fluxes of the primary and the secondary is correlated with the ditheirng positions. Different symbols represent different orbits.

Song, I., Schneider, G., Zuckerman, B., Farihi, J., Becklin, E. E.,  
Bessell, M. S., Lowrance, P., & Macintosh, B. A. 2006, ApJ,  
652, 724